JOURNAL OF BACTERIOLOGY, Apr. 1993, p. 2292–2303
0021-9193/93/082292-12$02.00/0

Vol. 175, No. 8

Expression of the *Rhodobacter sphaeroides hemA* and *hemT* Genes, Encoding Two 5-Aminolevulinic Acid Synthase Isozymes

ELLEN L. NEIDLE† AND SAMUEL KAPLAN*

Department of Microbiology and Molecular Genetics, University of Texas Health Science Center at Houston, P.O. Box 20708, Houston, Texas 77225

Received 19 November 1992/Accepted 15 February 1993

The nucleotide sequences of the *Rhodobacter sphaeroides hemA* and *hemT* genes, encoding 5-aminolevulinic acid (ALA) synthase isozymes, were determined. ALA synthase catalyzes the condensation of glycine and succinyl coenzyme A, the first and rate-limiting step in tetrapyrrole biosynthesis. The *hemA* and *hemT* structural gene sequences were 65% identical to each other, and the deduced HemA and HemT polypeptide sequences were 53% identical, with an additional 16% of aligned amino acids being similar. HemA and HemT were homologous to all characterized ALA synthases, including two human ALA synthase isozymes. In addition, they were evolutionarily related to 7-keto-8-aminopelargonic acid synthetase (BioF) and 2-amino-3-ketobutyrate coenzyme A ligase (Kbl), enzymes which catalyze similar reactions. Two *hemA* transcripts were identified, both expressed under photosynthetic conditions at levels approximately three times higher than those found under aerobic conditions. A single transcriptional start point was identified for both transcripts, and a consensus sequence at this location indicated that an Fnr-like protein may be involved in the transcriptional regulation of *hemA*. Transcription of *hemT* was not detected in wild-type cells under the physiological growth conditions tested. In a mutant strain in which the *hemA* gene had been inactivated, however, *hemT* was expressed. In this mutant, *hemT* transcripts were characterized by Northern (RNA) hybridization, primer extension, and ribonuclease protection techniques. A small open reading frame of unknown function was identified upstream of, and transcribed in the same direction as, *hemA*.

Rhodobacter sphaeroides is a metabolically versatile facultative photosynthetic bacterium with varied growth and biosynthetic capabilities (10). It can synthesize three kinds of tetrapyrroles: bacteriochlorophylls, hemes, and corrinoids. Depending on the physiological condition, the relative amounts of the different tetrapyrroles vary greatly (22). Bacteriochlorophyll is the predominant tetrapyrrole formed during photosynthetic growth, and its synthesis responds to environmental factors such as oxygen tension and light intensity. Although the early portion of the biosynthetic pathway is common to all tetrapyrroles, bacteriochlorophyll production can be repressed without interrupting heme or corrinoid production and without the accumulation of intermediates, even transiently (10, 22).

The first committed precursor in the common tetrapyrrole pathway is 5-aminolevulinate (ALA), and its formation is rate limiting (21, 22). In *R. sphaeroides*, as in some other bacteria, fungi, protozoa, and animals, the condensation of glycine and succinyl coenzyme A (succinyl-CoA) is mediated by the enzyme ALA synthase (succinyl-CoA:glycine *C*-succinyl transferase [decarboxylating], EC 2.3.1.37) (2). In a previous report from our laboratory, the existence of two ALA synthase isozymes in *R. sphaeroides* was suggested (47). In this study, nucleotide sequence determination confirmed that two genes, *hemA* and *hemT*, each encode a distinct ALA synthase. Questions have previously arisen concerning the number, nature, and cellular location of ALA synthases in *R. sphaeroides* (9, 17, 35, 36, 39, 42, 48, 52, 59). By characterizing the expression of *hemA* and *hemT*, we are now able to address some of these questions concerning the specific function of each gene in tetrapyrrole biosynthesis.

Genes encoding ALA synthases in several bacteria have been characterized (5, 15, 20, 25, 26, 32). Although ALA synthase isozymes are found in some vertebrates (14), no previous examples of bacterial isozymes have been reported. *Rhodobacter capsulatus*, a bacterium related to *R. sphaeroides*, encodes a single ALA synthase (5, 20). In most bacteria, as in plants, ALA is formed by a different biosynthetic route in which a glutamyl-tRNA intermediate is involved (2, 21). *Euglena gracilis* utilizes both pathways, and interesting evolutionary questions are raised by these findings (53). In this study, HemA and HemT were found to be homologous to each other and to all previously characterized ALA synthases, suggesting common evolutionary origins. In addition, the ALA synthases are evolutionarily related to two enzymes which catalyze similar reactions, 2-amino-3-ketobutyrate CoA ligase (acetyl-CoA:glycine *C*-acetyltransferase; EC 2.3.1.29) (Kbl) (1) and 7-keto-8-amino pelargonic acid synthase (BioF) (40).

MATERIALS AND METHODS

Bacterial strains, plasmids, and growth conditions. Bacterial strains and plasmids are listed in Table 1. *R. sphaeroides* strains were grown with Sistrom's succinic acid minimal medium (27), supplemented as needed with antibiotics at the following concentrations: tetracycline, 1 μg/ml; streptomycin, 50 μg/ml; spectinomycin, 50 μg/ml; and kanamycin, 25 μg/ml. *R. sphaeroides* cultures were grown aerobically at 30°C either on a rotary shaker or sparged with 30% O_2–69% N_2–1% CO_2. Photoheterotrophic cultures were grown in the light (10 W/m^2) either in completely filled screw-cap tubes or

* Corresponding author.
† Present address: Isogenetics, Inc., Chicago, IL 60612.

TABLE 1. Bacterial strains and plasmids

Organism and strain or plasmid	Relevant characteristic(s)	Reference or source
E. coli		
JM101	*supE thi* Δ(*lac-proAB*) F′ *traD36 proAB lacI*^{q}ZΔM15	34
DH5α	*supE44* Δ*lacU169* (ϕ80 *lacZ* ΔM15) *hsdR17 recA1 endA1 gyrA96 thi-1 relA1*	3
R. sphaeroides		
2.4.1	Wild type	50
HemA1	2.4.1 derivative, *hemA*::Ω Kn^r	37
HemT1	2.4.1 derivative, *hemT*::Ω Sm^r Sp^r	37
HemAT1	2.4.1 derivative, *hemA*::Ω Kn^r and *hemT*::Ω Sm^r Sp^r	37
Plasmids		
pBS	Ap^r, with T3 and T7 promoters	Stratagene
pUI551, pUI552	3.1-kb *hemT Sal*I fragment	47
pUI553, pUI554	7.0-kb *hemA Sal*I fragment	47
pUI1038	530-bp *Bgl*II-*Xho*I *hemT* fragment in pBS	This study (Fig. 8c)
PUI1042	565-bp *Nae*I-*Sac*I *hemA* fragment in pBS	This study (Fig. 7c)
pUI1044	147-bp *Fsp*I-*Sac*II ORFA fragment in pBS	This study

sparged with 95% N_2–5% CO_2. Strain HemAT1 was grown with ALA added at a final concentration of 0.2 mM. *Escherichia coli* strains were grown at 37°C with Luria broth (30) supplemented as needed with antibiotics at the following concentrations (per milliliter): 10 μg of tetracycline, 25 μg of streptomycin, 50 μg of spectinomycin, and 50 μg of ampicillin. Isopropyl-β-D-thiogalactoside (40 μM) and 5-bromo-4-chloro-3-indolyl-β-D-galactoside (30 μg/ml) were used to monitor β-galactosidase activity in the construction of plasmids. Cell growth was monitored turbidometrically with a Klett-Summerson colorimeter.

Generation, deletion, and DNA sequence determination of subclones. DNA fragments with sizes of 0.1 to 2.5 kb were cloned into M13mp18 and M13mp19 vectors (51, 58). Nested deletion derivatives of the larger fragments were generated by using the Cyclone I Biosystem of International Biotechnologies, Inc. (New Haven, Conn.). According to the manufacturer's instructions, the single-stranded ends of cloned DNA fragments were progressively digested by T4 DNA polymerase, and overlapping clones entirely covering both strands of the *hemA* and *hemT* regions were isolated. M13 bacteriophages were isolated, propagated, and used for the generation of single-stranded DNA sequencing templates (4). The DNA sequence was determined by the dideoxy chain termination method (43) with commercial kits from United States Biochemical Corp. (Cleveland, Ohio). α-^{35}S-dATP (>1,000 Ci/mmol) was purchased from the Amersham Corp. (Arlington Heights, Ill.). Sequencing reaction mixtures were electrophoretically separated on 8% polyacrylamide gels with 42% urea in Tris-borate-EDTA buffer prior to vacuum drying and autoradiography.

DNA sequence analysis. Computer programs from PC/GENE (IntelleGenetics, Inc., Mountainview, Calif.) and from the University of Wisconsin Genetics Computer Group software package were used (13). The SwissProt (release 22), EMBL (release 31), and GenBank (release 72) data bases were screened for sequence similarities with algorithms based on that of Lipman and Pearson (28).

Plasmid constructions, DNA isolations, and generation of ^{32}P-labeled probes. Plasmids and DNA fragments were isolated, treated with modifying enzymes, and electrophoretically analyzed by standard techniques (30). Recombinant plasmids were maintained in *E. coli* host strains (Table 1). Radioactive DNA or RNA probes using [α-^{32}P]dCTP (3,000 Ci/mmol) or [α-^{32}P]CTP (800 Ci/mmol) (Amersham Corp.) were made and utilized according to the manufacturers' instructions with nick translation systems (Bethesda Research Laboratories, Gaithersburg, Md.), random-primed DNA labeling kits (Boehringer Mannheim Biochemicals, Indianapolis, Ind.), or RNA transcription kits (Stratagene, La Jolla, Calif.). Deoxyoligonucleotides (30-mers from Genosys Biotechnologies, Inc., The Woodlands, Tex.) were labeled at the 5′ ends with [γ-^{32}P]ATP (6,000 Ci/mmol) as previously described (24). Unincorporated nucleotides were removed from labeled probes with Nuctrap push columns (Stratagene).

RNA isolations and Northern hybridization techniques. RNA was isolated from *R. sphaeroides* cultures when they reached an approximate cell density of 10^9 cells per ml grown photoheterotrophically or a density of 5×10^8 cells per ml grown aerobically. Two methods were used in the purification of total RNA: the method of Zhu and Kaplan (60) and a second method based on that of Sarmientos et al. (44). In this second method, cells from a growing culture (8 to 64 ml) were transferred to a flask in a boiling water bath containing lysis buffer (500 mM sodium acetate, 200 mM EDTA, and 5% sodium dodecylsulfate; 4:1 [vol/vol] ratio of cells to lysis buffer). The lysate was immediately added to hot phenol at 68°C, moved to an ice bath for several minutes, and then centrifuged at 5°C. The RNA was extracted an additional one or two times with phenol and once with phenol:chloroform:isoamyl alcohol (25:24:1). The RNA was precipitated overnight at 4°C with LiCl, 2 M final concentration. The RNA was pelleted, washed with 2 M LiCl, and suspended in water. It was then ethanol precipitated with sodium acetate, washed with 70% ethanol, and suspended in 0.5 ml of 50 mM Tris-chloride–5 mM $MgCl_2$. Residual DNA was removed with 10 U of RNase-free DNase I at 37°C for 20 min. Protein was removed by phenol extraction, and the RNA was recovered by ethanol precipitation. Finally, the RNA was dissolved in H_2O at a concentration of 1 to 5 mg/ml. Approximately 200 μg of RNA was obtained from 64 ml of cells.

RNA concentrations were determined both by orcinol

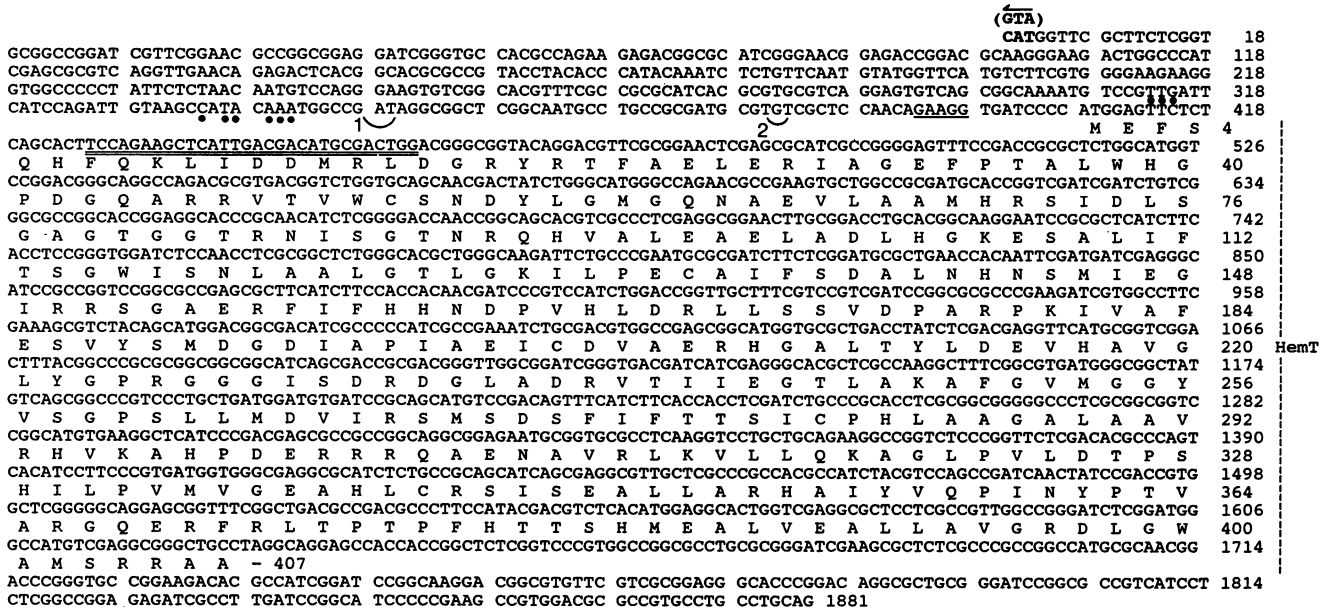

FIG. 1. DNA sequence of the chromosomal *hemT* region. Below the *hemT* coding region is the deduced amino acid sequence of its gene product. A possible Shine-Dalgarno (46) ribosome binding site is underlined. An oligodeoxynucleotide complementary to the 30 double-underlined nucleotides at the 5′ region of *hemT* was used in Northern hybridization and primer extension studies. The translation initiation codon of the *rdxA* gene (38), which is transcribed in the opposite direction to *hemT*, is indicated in parentheses. Regions labeled 1 and 2 were identified as transcript initiation sites by primer extension studies (Fig. 8). Closed circles are shown below nucleotide sequences matching those in the promoter region of the *R. sphaeroides rrnB* operon (16).

assays and by A_{260} (8). RNA was electrophoretically separated on agarose-formaldehyde gels (30) with 2 to 8 μg of RNA per lane. RNA was transferred by capillary action to nylon membranes (MagnaGraph; pore size, 0.45 μm; Micron Separations, Inc., Westborough, Mass.) (30), and a UV cross-linker was used to bind the RNA to the membranes (UVC 1000; Hoefer Scientific Instruments, San Francisco, Calif.). Approximate sizes of the mRNAs were estimated by using RNA standards (Bethesda Research Laboratories Life Technologies, Inc., Gaithersburg, Md.), which, following transfer to the nylon membranes, were stained with methylene blue dye (30). High-stringency hybridization and wash conditions were used with labeled DNA and RNA probes. Hybridization protocols were provided by the manufacturer of the RNA transcription procedure used to generate RNA probes (Stratagene). Hybridizations and washes with RNA probes were done at 65°C. Hybridizations with end-labeled oligonucleotide probes were done at 62°C, with final washes at 45°C. All other DNA probes were hybridized at 45°C, with wash temperatures of 55°C. Radioactive signals were quantitated with a Betascope 603 Blot Analyzer (Betagen Corp., Waltham, Mass.). Some signals were normalized relative to those generated by probes specific for rRNA.

Ribonuclease protection assays. Ribonuclease protection assays were done according to the directions for a commercial kit (RPA II; Ambion, Austin, Tex.). Single-stranded RNA probes were gel purified and hybridized overnight at 45°C with 10 to 30 μg of total RNA. The supplied mixture of RNase A and RNase T1 was used in a 1:100 dilution at 37°C for 30 min to digest unprotected single-stranded RNA. Protected fragments were recovered by precipitation and were resolved on 5% polyacrylamide gels containing 8 M urea. An RNA template set (Ambion) was used to generate ^{32}P-labeled size standards of 100 to 500 nucleotides in length.

Primer extension analysis. End-labeled oligonucleotides were hybridized with 10 μg of total RNA and then used as templates in reactions with reverse transcriptase and deoxynucleotides as previously described (24). The same ^{32}P-labeled oligonucleotides were used in parallel sequencing reactions with appropriate single-stranded DNA templates. dGTP was incorporated in both the reverse transcriptase and sequencing reactions. In addition, the analog dITP was used to resolve difficulties in DNA sequence determination caused by the high G+C content of *R. sphaeroides* DNA.

Nucleotide sequence accession number. Nucleotide sequences in the *hemA* and *hemT* regions have been assigned GenBank accession numbers L07490 and L07489, respectively.

RESULTS

DNA sequence determination of the *hemA* and *hemT* genes. A 3.1-kb DNA fragment carrying *hemT* and a 7.0-kb DNA fragment carrying *hemA* were previously isolated from chromosomal DNA of *R. sphaeroides* wild-type 2.4.1 (47). The complete nucleotide sequence determination of the 3.1-kb *hemT* region has been described previously (38), and part of this sequence is presented in Fig. 1. The *hemA* gene was localized within the 7.0-kb region to two adjacent DNA fragments generated by restriction endonuclease *Bam*HI (37). These two fragments, one 2.5 kb and the other 1.2 kb in length, were each cloned into M13mp19 in both orientations relative to the vector sequences. The DNA sequences of both strands of the *Bam*HI fragments were completely determined. The junction sequence was confirmed by using a DNA fragment spanning the *Bam*HI border that was generated by restriction endonucleases *Bgl*II and *Sst*I. The

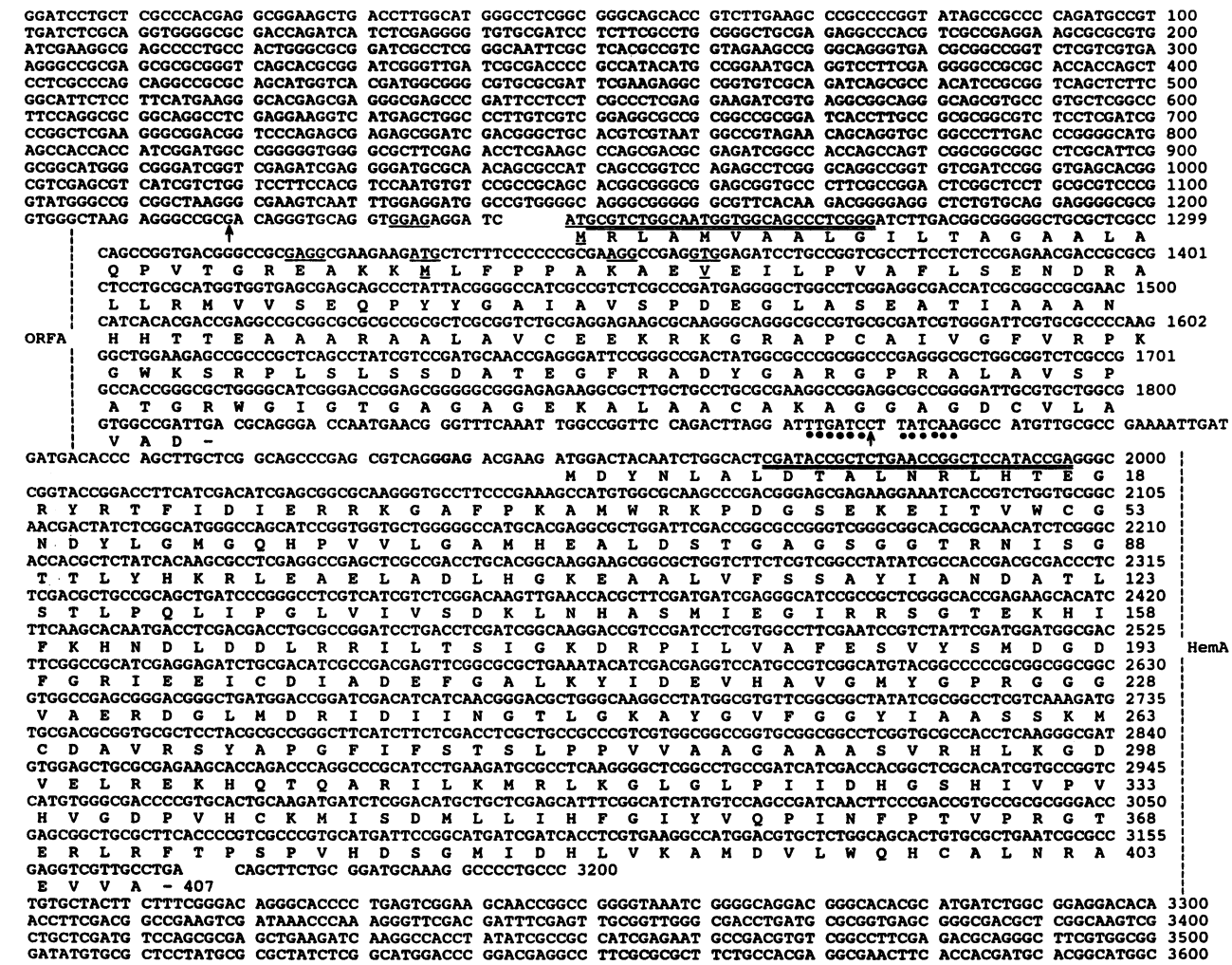

FIG. 2. DNA sequence of the *hemA* region encompassing two adjacent *Bam*HI-generated DNA fragments. The deduced amino acid sequence of the gene product is shown below the *hemA* coding region. A possible Shine-Dalgarno (46) ribosome binding site is indicated in bold type immediately upstream of *hemA*. An open reading frame of unknown function, ORFA, is indicated with the deduced amino acid sequence of a possible gene product. Potential ORFA initiator codons and Shine-Dalgarno ribosome binding sites which precede them are underlined. Oligodeoxynucleotides complementary to the sequences which are double-underlined at the 5′ regions of ORFA and *hemA* were used in Northern hybridization and primer extension studies. Arrows indicate transcript initiation sites upstream of ORFA and *hemA* that were identified by primer extension studies. Closed circles indicate nucleotides which match the *R. meliloti* or *E. coli* anaerobox consensus sequences for FixK/Fnr protein binding (Fig. 9).

nucleotide sequence of the 3.7-kb *hemA* region is presented in Fig. 2.

Comparisons of ALA synthase sequences. DNA sequence analyses revealed the locations of the *hemA* and *hemT* genes. Each structural gene is 1,224 nucleotides in length, and each is comprised of 407 codons (Fig. 1 and 2). In a comparison of the *hemA* and *hemT* sequences, 65% of the aligned nucleotides were identical. A comparison of the deduced amino acid sequences showed 53% identity between aligned HemA and HemT residues, with an additional 16% of the aligned residues being similar. The HemA and HemT proteins were predicted to have molecular masses of 44,558 and 44,332 Da, respectively. Both genes had a G+C content of 66 mol%, with similar codon usage in each.

Data base searches revealed HemA and HemT to be homologous to the single bacterial ALA synthases of *R. capsulatus* (5, 20), *Bradyrhizobium japonicum* (32), *Agrobacterium radiobacter* (15), and *Rhizobium meliloti* (for which only a partial sequence is available) (25, 26). In pairwise comparisons of complete ALA synthase sequences, identity between aligned residues ranged from 50 to 76%. The greatest similarity detected was between the HemA of *R. sphaeroides* and that of *R. capsulatus*; there was 76% identity and an additional 10% similarity between aligned residues. The resemblance between these two HemA sequences is significantly greater than that between HemA and HemT of *R. sphaeroides*.

Homologies were also detected between HemA and HemT and eukaryotic ALA synthases, including those of *Aspergillus nidulans* (7), yeast (49), chickens (29), mice (45), rats (56), and humans (6). The bacterial ALA synthases resemble the C-terminal portion of eukaryotic ALA synthases which comprise the mature proteins (14). An alignment of some of these sequences is shown in Fig. 3. In this

FIG. 3. Alignment of ALA synthase sequences from diverse sources. Bacterial ALA synthase sequences encoded by *R. sphaeroides hemA* (RsA), *R. capsulatus hemA* (RcA) (5, 20), *B. japonicum hemA* (BjA) (32), and *R. sphaeroides hemT* (RsT) are aligned with those encoded by eukaryotic genes from chicken, *Gallus gallus hem1* (Gg) (29), and humans, *Homo sapiens hem1* (H1) and *hem2* (H2) (6). The N-terminal portion of the eukaryotic proteins are proteolytically cleaved following import into the mitochondria and the sequences of these regions are not shown (. . .). Aligned residues identical in at least six of these sequences are enclosed in boxes. Residues conserved in all of these sequences as well as in those of BioF (19, 40) and Kbl (1) (Fig. 5) are indicated by asterisks. Residues likely to be involved in pyridoxal phosphate binding are indicated by open arrows and by a closed circle. Closed arrow heads show two cysteine residues conserved in all of the ALA synthase sequences.

alignment, 41% of the residues are identical in at least six of the seven sequences. Pairwise comparisons of the homologous regions of the ALA synthase isozymes of humans with those of *R. sphaeroides* showed 49 to 50% identity and 68 to 70% similarity between aligned residues.

Comparisons of HemA and HemT with BioF and Kbl. The gene product of the *bioF* gene of *Bacillus sphaericus* (19) and *E. coli* (40) and that of the *kbl* gene of *E. coli* (1) were also identified as homologs of HemA and HemT. The BioF enzyme, involved in biotin biosynthesis, mediates the condensation of alanine and pimelic acid-CoA to form 7-keto-8-amino pelargonic acid (19, 40). The Kbl enzyme, which may be involved in threonine metabolism, catalyzes the reversible cleavage-condensation reaction between 2-amino-3-ke-

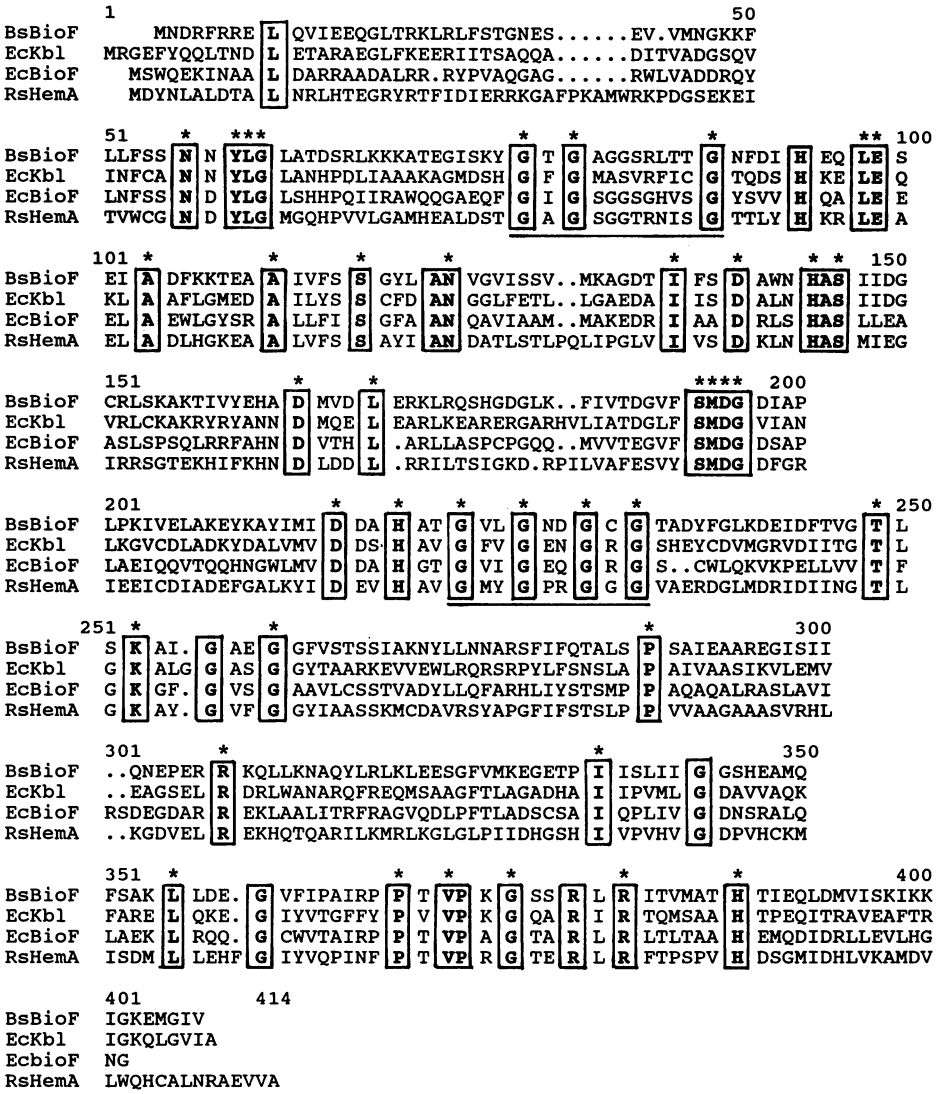

FIG. 4. Alignment of HemA, BioF, and Kbl deduced amino acid sequences. Aligned residues identical in *R. sphaeroides* HemA (RsHemA), *B. sphaericus* BioF (BsBioF) (19), *E. coli* Kbl (EcKbl) (1), and *E. coli* BioF (40) are enclosed in boxes. Of these residues, those conserved in all of the ALA synthase sequences shown in Fig. 4 are indicated by an asterisk. Two glycine-rich regions which could be involved in CoA (54) or pyridoxal phosphate (31) binding are underlined.

tobutyrate and glycine plus acetyl-CoA (1). The reactions catalyzed by these two enzymes are very similar to that catalyzed by ALA synthases. An alignment is shown in Fig. 4 of BioF, Kbl, and HemA sequences. Of the conserved ALA synthase residues enclosed in boxes in Fig. 3, 25% are also conserved in BioF and Kbl (Fig. 4).

Open reading frame analysis in the *hemA* region. An open reading frame, designated ORFA, (Fig. 2) was found immediately upstream of and transcribed in the same direction as *hemA*. Several possible ATG or GTG initiation codons were preceded by Shine-Dalgarno (46) ribosome binding sites (Fig. 2). A 15- to 19-kDa protein could be encoded, although the deduced amino acid sequence of the ORFA gene product was not homologous to any of those in the data bases.

Transcript analyses of *hemA* and *hemT* by Northern hybridization. RNA was analyzed from the wild-type and *hem* mutant strains. Strain HemA1 carries the Ω Kn^r cartridge within the chromosomal *hemA* structural gene (Fig. 5) (37). In strain HemT1 the chromosomal *hemT* gene is disrupted by the Ω Sm^r Sp^r cartridge (37). In strain HemAT1, both *hem* structural genes are inactivated (37). Labeled DNA from the 5′ end of *hemA* was used in Northern (RNA) hybridizations (Fig. 5), and similar results were obtained by using *hemA*-specific labeled RNA and labeled oligonucleotide probes (data not shown). Two *hemA* transcripts, 1.4 and 1.9 kb, were identified in RNA of the wild-type and HemT1 strains grown either aerobically or photosynthetically. The smaller of these transcripts was detected at levels twice those of the larger transcript, and both transcripts were expressed under photosynthetic conditions at levels three times higher than those under aerobic growth conditions.

In RNA of the HemA1 and HemAT1 mutants, a single shortened transcript with a length of 0.68 kb was found. The Ω cartridge insert in the *hemA* gene of these strains contains transcriptional termination signals at the beginning of the antibiotic resistance cassette (41), suggesting that transcrip-

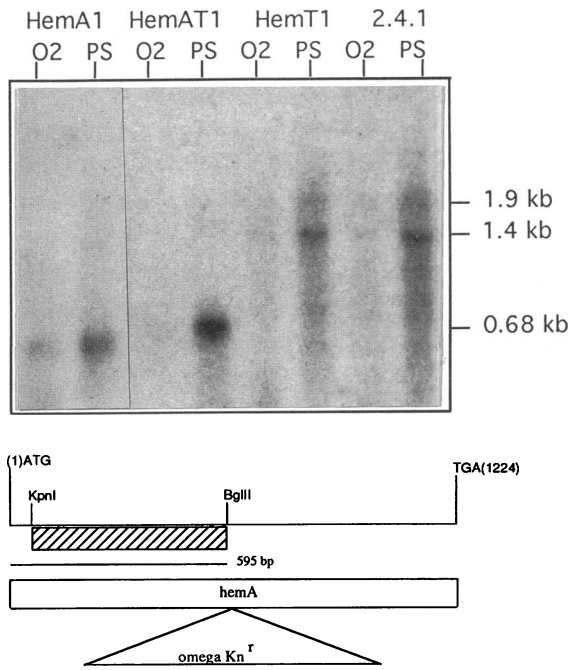

FIG. 5. Northern hybridization analysis of *hemA* transcripts. A labeled DNA probe (striped box) was used with RNA from wild-type, 2.4.1, and *hem* mutant strains (HemA1, HemAT1, and HemT1) grown aerobically (O2) or photoheterotrophically (PS). In each lane, 2 μg of total RNA was electrophoretically separated. The sizes corresponding to *hemA* transcripts are shown on the right. The *hemA* structural gene from the ATG translation initiation codon to the TGA termination codon is 1,224 bp in length. In the HemA1 and HemAT1 mutant strains, an omega Kn^r cartridge (41) disrupts *hemA* at nucleotide position 595.

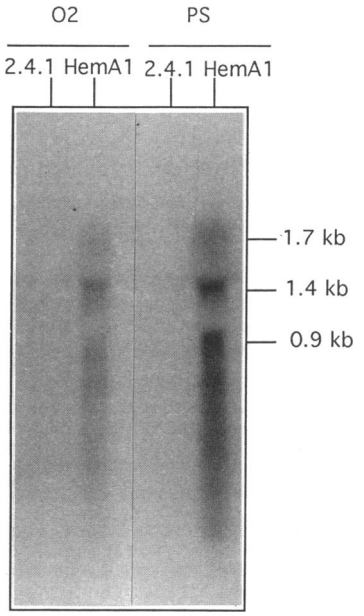

FIG. 6. Northern hybridization analysis of *hemT* transcripts. A *hemT*-specific labeled RNA probe (between the *Bgl*II and *Xho*I sites, Fig. 9c) was used with RNA from the wild-type 2.4.1 and *hemA* mutant HemA1. Strains were grown aerobically (O_2) or photoheterotrophically (PS). In each lane, 8 μg of total RNA was electrophoretically separated. The sizes of signals corresponding to transcripts are shown on the right.

tion initiates approximately 80 nucleotides upstream of *hemA*. Under photosynthetic conditions, the detected levels of the shortened *hemA* transcripts in strains HemA1 and HemAT1 were approximately three- to fivefold higher than those of the wild-type *hemA* transcripts. Under aerobic conditions, however, there were no elevated levels of a shortened *hemA* transcript in the *hemA* mutants relative to the wild-type full-length transcripts.

Three *hemT* transcripts, 1.7, 1.4, and 0.9 kb, were detected in RNA isolated from HemA1 grown either aerobically or photosynthetically (Fig. 6) with a *hemT*-specific RNA probe generated between *Xho*I and *Bgl*II restriction sites (see Fig. 8c). The *hemT* transcripts were present in photosynthetically grown cells at levels three times higher than those in aerobically grown cells. No *hemT* transcripts were detected in wild-type RNA (Fig. 6) or in RNA from HemT1 or HemAT1 grown either aerobically or photosynthetically (data not shown).

Mapping the 5′ ends of *hemA* transcripts by primer extension and ribonuclease protection assays. A ^{32}P-labeled oligonucleotide primer, complementary to the sequence double underlined in Fig. 2 at the 5′ end of *hemA*, was hybridized with 10 μg of total RNA. Transcript initiation sites were identified by primer extension with reverse transcriptase (Fig. 7a). The majority of *hemA* transcripts, from aerobically or photosynthetically grown cells, started 79 nucleotides upstream of the ATG-methionine translational initiation codon (indicated by arrows, Fig. 2 and 7a). The double bands observed at this position may be artifacts resulting from pausing of the reverse transcriptase (33). In addition, a second weaker signal was observed in the photosynthetic sample but not in the aerobic sample (Fig. 7a). Identical signals were detected with wild-type RNA (data not shown) and with RNA from strain HemA1 (Fig. 7a).

A single fragment of approximately 360 nucleotides in length was identified with a *hemA*-specific RNA probe following hybridization to wild-type RNA and ribonuclease digestion (Fig. 7b and c). The same result was found with RNA isolated from the HemA1, HemT1, and HemAT1 mutants (data not shown). These results predict a single major transcriptional start site 65 ± 20 nucleotides upstream of the *hemA* translational initiation codon (Fig. 7c).

Mapping the 5′ ends of *hemT* transcripts by primer extension and ribonuclease protection assays. A ^{32}P-labeled oligonucleotide primer, complementary to the *hemT* sequence doubly underlined in Fig. 1, was used in primer extension studies of wild-type and HemA1 RNA. Multiple band patterns were observed in reactions with RNA from HemA1 (Fig. 8a), and no signals at all were detected with wild-type RNA (data not shown). The HemA1 band patterns were identical for aerobically and photosynthetically grown cells. The majority of signals would indicate transcription initiation in two main regions (labeled 1 and 2 in Fig. 1 and 8a), one approximately 25 nucleotides upstream of the *hemT* translational ATG start signal and the other approximately 60 nucleotides upstream of the ATG codon.

With a *hemT*-specific RNA probe (Fig. 8c), two protected fragments were identified following hybridization to HemA1 RNA and ribonuclease digestion (Fig. 8b). The sizes of these fragments were 100 and 125 nucleotides. Aerobically or photosynthetically grown cells yielded the same results (data not shown). These results predict two transcription initiation sites, one 25 ± 10 and the other 50 ± 10 nucleotides

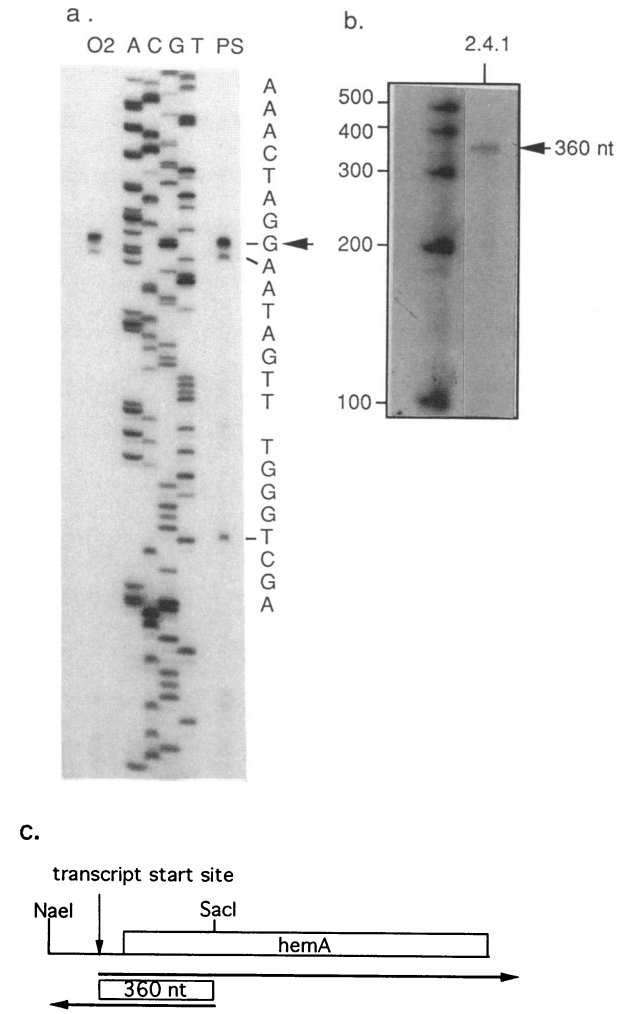

FIG. 7. 5'-end mapping of *hemA* transcripts. (a) Primer extensions with a *hemA*-specific oligonucleotide (Fig. 2) and RNA from strain HemA1 grown aerobically (O_2) or photoheterotrophically (PS). The same ^{32}P-labeled oligonucleotide was used to generate the sequencing ladder (lanes A, C, G, and T). The arrow indicates the major *hemA* transcript initiation site on the corresponding DNA sequence of the coding strand. This site is 79 nucleotides upstream of the *hemA* ATG translation initiation codon. An additional signal found in the RNA of only photoheterotrophically grown cells is indicated. (b) Ribonuclease protection assay with 10 μg of RNA from photoheterotrophically grown wild-type strain 2.4.1 and a labeled RNA probe, described below. An approximately 360-nucleotide protected fragment was detected (arrow). The sizes (in nucleotides [nt]) of labeled RNA standards are indicated. (c) Depiction of the RNA probe (leftward arrow between *Nae*I and *Sac*I restriction sites) which hybridized to *hemA* transcripts (rightward arrow), yielding a 360-nucleotide protected fragment after ribonuclease digestion of single-stranded RNA. The same location of a major transcript start site (downward arrow) was deduced by the methods used for the results shown in panels a and b.

upstream of the *hemT* translation-initiation codon. No protected fragments were observed with the *hemT* probe and 30 μg of wild-type, HemT1, or HemAT1 RNA (Fig. 8b).

Identification of an ORFA transcript. A probe internal to the ORFA coding region, generated from pUI1044 (Table 1), identified a 0.7-kb wild-type transcript by Northern hybridization analysis (data not shown). A transcription initiation site was found upstream of ORFA by primer extension studies with a ^{32}P-labeled oligonucleotide primer complementary to the ORFA sequence doubly underlined in Fig. 2 (data not shown). The location of this site is indicated by an arrow in Fig. 2, and it was the same in RNA isolated from aerobically and photosynthetically grown cells.

Sequences that may be involved in transcriptional regulation. Upstream of *hemA*, a sequence matching the consensus sequence used to bind the transcriptional regulators Fnr and FixK was found (Fig. 9A) (11, 46b). A good match for this consensus sequence is found upstream of the *hemA* gene of *B. japonicum* (11, 32). The locations of these putative regulatory regions relative to the *hemA* genes and transcripts are shown in Fig. 9B. No sequences similar to the consensus were found upstream of *R. sphaeroides hemT* or *R. capsulatus hemA* (5, 20). Upstream of what appears to be the major *hemT* transcript initiation site are nucleotides (indicated by circles in Fig. 1) whose sequence and spacing match those of the promoter region upstream of the *R. sphaeroides rrnB* operon (16).

DISCUSSION

Sequence comparisons suggest structurally and functionally important regions of HemA and HemT. The HemA and HemT predicted molecular weights are in good agreement with previous characterizations of ALA synthase from *R. sphaeroides* (21, 36). In past studies, however, the presence of isozymes and/or multiple forms of the enzyme was not correlated with particular gene products (9, 17, 39, 42, 48, 52, 59). There are two similarly sized but immunologically distinct ALA synthases in *R. sphaeroides* subsp. *denitrificans*, and although the 2.4.1 wild-type *R. sphaeroides* strain used in these studies is not capable of nitrate respiration, HemA and HemT may be homologs of the isozymes described by Michalski and Nicholas (35). A high degree of homology was detected between all ALA synthases examined, including those from such diverse sources as humans and bacteria (Fig. 3). In the eukaryotic ALA synthases, the N-terminal peptide sequence is cleaved following mitochondrial import (14). It is interesting that bacteria which utilize ALA synthase have previously been suggested to be the evolutionary origin of the mitochondrial organelles (57).

E. coli forms ALA by a different biosynthetic pathway (2) and therefore does not encode ALA synthase. It does, however, encode two enzymes, Kbl (1) and BioF (40), which are evolutionarily related to ALA synthase. Common functions of these enzymes include the binding of pyridoxal 5'-phosphate (PLP) and a CoA-bound substrate. The conserved lysine residue indicated by an arrow in Fig. 3 (Fig. 4, position 251) is likely to be involved in enzyme-PLP-Schiff base formation (40). The region of an ALA synthase amino acid substitution causing human sideroblastic anemia (marked by a circle in Fig. 3) has also been implicated in PLP binding (12). In two different regions of the sequence alignments, several glycines are conserved among all sequences (underlined in Fig. 4). Although the spacings of these residues differ from previously identified motifs, glycine-rich regions bind both dinucleotide-containing cofactors (54) and PLP (31). Glycines may be used to bind CoA and PLP. It is possible that cysteine residues play a role in the activation of ALA synthases from *R. sphaeroides* (21, 22, 39, 42, 48), and two cysteines are conserved in all of the ALA synthases (Fig. 3).

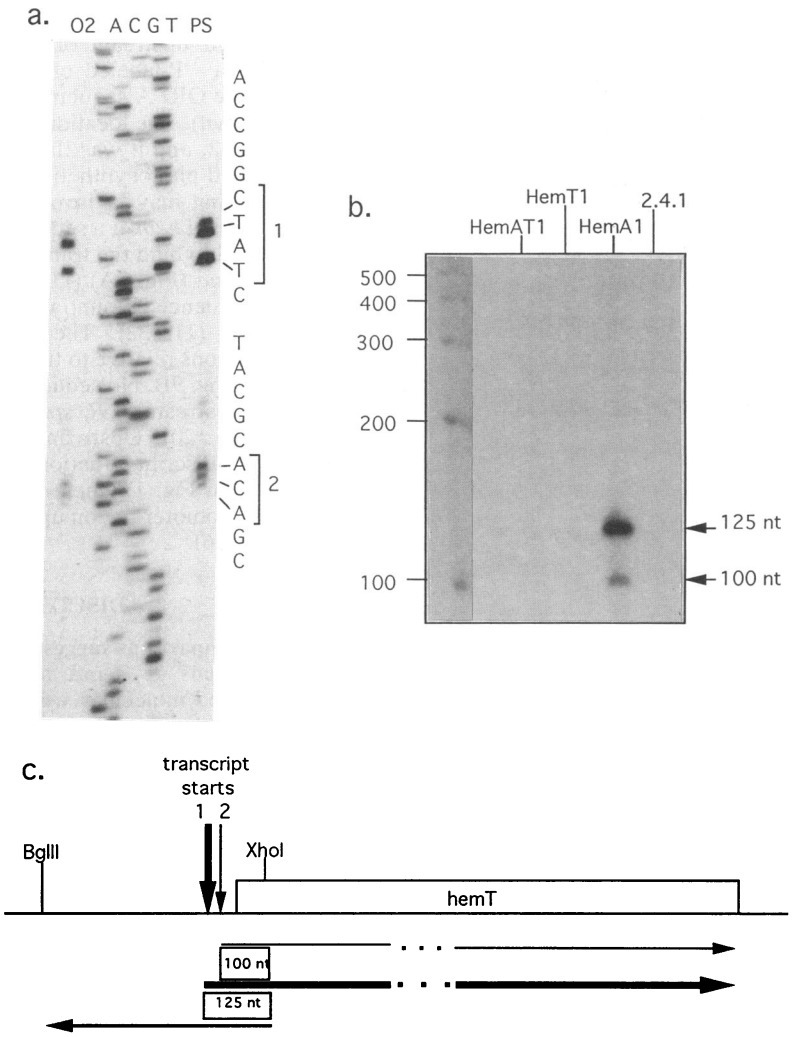

FIG. 8. 5′-end mapping of *hemT* transcripts. (a) Primer extensions with a *hemT*-specific oligonucleotide (Fig. 2) and RNA from aerobically (O_2) or photoheterotrophically (PS) grown strain HemA1. The same primer was used to generate the sequencing ladder (lanes A, C, G, and T). Two regions of transcripts initiation are shown in brackets (1 and 2) adjacent to the corresponding DNA sequence of the *hemT* coding strand. (b) Ribonuclease protection assays with 30 μg each of RNA from photoheterotrophically grown strains HemAT1, HemT1, HemA1, and 2.4.1 and a labeled RNA probe (see below). Arrows point to two protected fragments from RNA of HemA1. The sizes (in nucleotides [nt]) of labeled RNA standards are given. (c) Depiction of the RNA probe (leftward arrow between *Xho*I and *Bgl*II restriction sites) used to hybridize with *hemT* transcripts (rightward arrows), not drawn to scale (. . .). Transcript start sites (downward arrows 1 and 2) at locations approximately 60 and 25 nucleotides upstream of the *hemT* ATG initiation codon correspond to regions 1 and 2 of the primer extensions (panel a) and to the 5′ regions of the 125- and 100-nucleotide fragments detected by ribonuclease protection assays (panel b).

Specific roles of ALA synthase isozymes. In humans, ALA synthase isozymes are regulated in a tissue-specific manner; ALA synthase 1 is responsible for general tetrapyrrole biosynthesis in all tissues, whereas ALA synthase 2 meets the increased demand for hemes in erythroid tissues (6, 12, 14). The two enzymes and the corresponding genes are differentially regulated, and the genes are located on different chromosomes. *R. sphaeroides* is the only bacterium in which ALA synthase isozymes have been found. The complex regulation of tetrapyrrole biosynthesis in *R. sphaeroides* had led to the hypothesis of a bacteriochlorophyll-specific ALA synthase (22). In this report, however, characterization of *hemA* and *hemT* indicates that neither gene is expressed specifically in response to the increased photosynthetic demand for bacteriochlorophyll. The genes are, however, located on different chromosomes and are clearly subject to different regulation. In *R. sphaeroides* subsp. *denitrificans*, the relative level of each ALA synthase isozyme is affected by the presence of nitrate in the growth medium, but neither enzyme was found to have a distinct denitrifying or photosynthetic physiological function (35).

Characterization of *hemA* and *hemT* transcripts. Under the physiological conditions tested, evidence for the expression of *hemA* but not *hemT* was found in the wild-type strain 2.4.1. In the HemA1 mutant, however, *hemT* was expressed under both aerobic and photoheterotrophic conditions. Under photoheterotrophic growth conditions, a wild-type copy of *hemA* carried in *trans* in strain HemA1 reduced the level of *hemT* expression by 75% (38a). It is possible that *hemT* is normally expressed under physiological conditions which have not been tested in these studies. Questions of mRNA abundance and stability have not been addressed in this

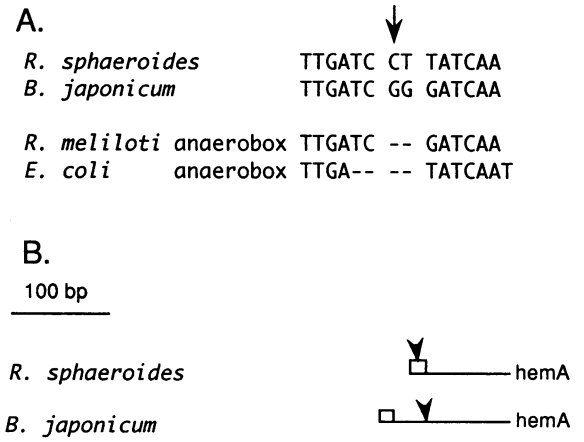

FIG. 9. Possible regulatory sequences upstream of *hemA*. (A) Sequences upstream of *hemA* in *R. sphaeroides* and *B. japonicum* (32) match the anaerobox consensus sequences for binding the transcriptional regulatory proteins Fnr and FixK (11, 46a). The arrow shows the transcript initiation site of *R. sphaeroides*. (B) Depiction of the relative locations of the *hemA* genes, transcript initiation sites (arrowheads), and anaerobox consensus sequences (boxes).

report, and these factors may also contribute to our inability to detect *hemT* transcripts in the wild-type 2.4.1 strain.

The sizes of the wild-type *hemA* transcripts, 1.4 and 1.9 kb, would suggest that additional genes are not coexpressed with the 1.2-kb *hemA*, although it is possible that the larger transcript could include a small downstream coding region. The downstream region has not been explored, but a small open reading frame of unknown function upstream of *hemA* was independently expressed. The major *hemA* transcript initiation site was identified. In addition a primer extension signal, of unknown significance, was observed by using RNA from photosynthetically but not aerobically grown cells (Fig. 7a). No corresponding transcription-initiation site was identified in ribonuclease protection assays, nor was a photosynthetic-specific transcript identified in Northern hybridizations.

Three *hemT* signals were identified by Northern hybridization analysis of strain HemA1 RNA (Fig. 6). The 0.9-kb signal is not large enough to encompass the entire 1.2-kb *hemT* structural gene, and it may represent mRNA breakdown products. Preliminary results suggest that all *hemT* transcripts are very unstable (38a). Two main transcript start sites were identified. The relative intensity of signals suggests that the 1.4-kb *hemT* transcript initiates approximately 60 nucleotides upstream of the ATG translation-initiation codon and that the 1.7-kb *hemT* transcript initiates approximately 25 nucleotides upstream of this ATG codon (Fig. 8). The multiple bands observed in primer extension analyses of the *hemT* transcripts may be related to the high G+C content in this region, although further work is needed to determine whether there are multiple transcript start sites within this area.

Transcriptional regulation of *hemA* and *hemT*. In the wild-type and the HemT1 mutant, *hemA* was expressed photosynthetically at three times the aerobic levels. In addition, *hemT* photosynthetic transcript levels compared with aerobic transcript levels were threefold higher in the HemA1 mutant. A similar increase in *R. capsulatus hemA* promoter activity was found in *hemA-lacZ* fusion studies when oxygen tension in the culture medium was lowered (55). The increased transcription corresponds to a comparable photosynthetic increase in *R. sphaeroides* ALA synthase enzyme activity, as measured in vitro (37). This level of *hemA* and *hemT* transcriptional regulation, however, is not sufficient to account for the great increases in bacteriochlorophylls, relative to hemes, that occur under photosynthetic growth conditions (10, 22). Previous studies have indicated that ALA synthase activity is also regulated posttranslationally (21, 22).

In the HemAT1 mutant, under photosynthetic conditions, ALA added to the culture medium is not sufficient to produce wild-type levels of bacteriochlorophyll (37). Under these conditions of bacteriochlorophyll limitation, the transcriptional response in HemAT1 may be increased expression of *hemA*, consistent with the high levels of a shortened mutant *hemA* transcript found. In the HemAT1 mutant, no shortened *hemT* transcript was detected at all despite the use of probes specific for the 5′ region of the transcript.

Possible DNA transcriptional regulatory sequences. The *hemA* transcription initiation site is located within a short region matching the consensus sequence for binding the transcriptional regulators Fnr and FixK (Fig. 9) (11, 46b). Although these regulators have not been identified in *R. sphaeroides*, a similar consensus binding sequence is found upstream of the oxygen- and light-regulated *puc* operon (23). The location of the potential binding region relative to the 5′ end of *hemA* transcripts suggests that an Fnr or FixK-type protein would act as a repressor in *R. sphaeroides* (Fig. 9b). It is interesting to note that in *R. meliloti*, potential Fnr or FixK-binding sites are found upstream of the *fixK* gene and also upstream of the *fixLJ* genes which encode a two-component regulatory system which responds to oxygen levels through a heme moiety of the FixL protein (11, 18, 46a). The possibility that in *R. sphaeroides* an Fnr or FixK homolog could affect heme formation and hemoprotein regulation through expression of ALA synthase needs to be tested.

No Fnr or FixK-binding site was found upstream of *hemT*. The region upstream of *hemT* may serve to regulate expression of both *hemT* and *rdxA*, a gene which encodes a membrane protein likely to have oxidation-reduction functions (38). Upstream of the main *hemT* transcript initiation site were sequences like those in the promoter region of the *R. sphaeroides rrnB* operon (16).

ACKNOWLEDGMENTS

We thank Jeong K. Lee and Paul E. Hessler for assistance with RNA isolations and techniques and Sylvia C. Dryden for assistance with DNA sequence determination.

This work was supported by Public Health Service grant GM31667-07 to S.K. from the National Institutes of Health and by National Research Service Award GM13138 to E.L.N. from the National Institutes of Health.

REFERENCES

1. **Aronson, B. D., P. D. Ravnikar, and R. L. Somerville.** 1988. Nucleotide sequence of the 2-amino-3-ketobutyrate coenzyme A ligase (*kbl*) gene of *E. coli*. Nucleic Acids Res. **16**:3586.
2. **Avissar, Y. J., J. G. Ormerod, and S. I. Beale.** 1989. Distribution of δ-aminolevulinic acid biosynthetic pathways among phototrophic bacterial groups. Arch. Microbiol. **151**:513–519.
3. **Bethesda Research Laboratories.** 1986. BRL pUC host: *E. coli* DH5α™ competent cells. Bethesda Res. Lab. Focus **8**:9–10.
4. **Bethesda Research Laboratories.** 1989. M13 cloning/dideoxy sequencing instruction manual. Bethesda Research Laboratories, Inc., Gaithersburg, Md.

5. **Biel, S. W., M. S. Wright, and A. J. Biel.** 1988. Cloning of the *Rhodobacter capsulatus hemA* gene. J. Bacteriol. **170:**4832–4834.
6. **Bishop, D. F.** 1990. Two different genes encode δ-aminolevulinate synthase in humans: nucleotide sequences of cDNAs for the housekeeping and erythroid genes. Nucleic Acids. Res. **18:**7187–7188.
7. **Bradshaw, R. E., S. W. C. Dixon, D. C. Raitt, and T. M. Pillar.** 1992. Sequence submitted to EMBL and GenBank.
8. **Clark, J. M., and R. L. Switzer.** 1977. Experimental biochemistry, 2nd ed., p. 207–218. W. H. Freeman & Co., San Francisco.
9. **Clement-Metral, J. D.** 1979. Activation of ALA synthase by reduced thioredoxin in *Rhodopseudomonas sphaeroides* Y. FEBS Lett. **101:**116–120.
10. **Cohen-Bazire, G., W. R. Sistrom, and R. Y. Stanier.** 1956. Kinetic studies of pigment synthesis by non-sulfur purple bacteria. J. Cell. Comp. Physiol. **49:**25–68.
11. **Colonna-Romano, S., W. Arnold, A. Schluter, P. Boistard, A. Puhler, and U. B. Priefer.** 1990. An Fnr-like protein encoded in *Rhizobium leguminosarum* biovar *viciae* shows structural and functional homology to *Rhizobium meliloti* FixK. Mol. Gen. Genet. **223:**138–147.
12. **Cotter, P. D., M. Baumann, and D. F. Bishop.** 1992. Enzymatic defect in "X-linked" sideroblastic anemia: molecular evidence for erythroid δ-aminolevulinate synthase deficiency. Proc. Natl. Acad. Sci. USA **89:**4028–4032.
13. **Devereux, J., P. Haeberli, and O. Smithies.** 1984. A comprehensive set of sequence analysis programs for the VAX. Nucleic Acids Res. **12:**387–395.
14. **Dierks, P.** 1990. Molecular biology of eukaryotic 5-aminolevulinate synthase, p. 201–234. *In* H. A. Dailey (ed.), Biosynthesis of hemes and chlorophylls. McGraw-Hill, New York.
15. **Drolet, M., and A. Saserman.** 1991. Cloning and nucleotide sequence of the *hemA* gene of *Agrobacterium radiobacter*. Mol. Gen. Genet. **226:**250–256.
16. **Dryden, S. C.** 1992. Identification and characterization of the ribosomal RNA operons from *Rhodobacter sphaeroides*. Ph.D. dissertation. University of Illinois, Urbana-Champaign.
17. **Fanica-Gaignier, M., and J. Clement-Metral.** 1973. Cellular compartmentation of two species of δ-aminolevulinic acid synthetase in a facultative photoheterotrophic bacterium (*Rps. spheroides Y.*). Biochem. Biophys. Res. Commun. **55:**610–615.
18. **Giles-Gonzalez, M. A., G. S. Ditta, and D. R. Helinski.** 1991. A haemoprotein with kinase activity encoded by the oxygen sensor of *Rhizobium meliloti*. Nature (London) **350:**170–172.
19. **Gloeckler, R., I. Ohsawa, D. Speck, C. Ledoux, S. Bernard, M. Zinsius, D. Villeval, T. Kisou, K. Komogawa, and U. Lemoine.** 1990. Cloning and characterization of the *Bacillus sphaericus* genes controlling the bioconversion of pimelate into dethiobiotin. Gene **87:**63–70.
20. **Hornberger, U., R. Liebetanz, H. V. Tichy, and G. Drews.** 1990. Cloning and sequencing of the *hemA* gene of *Rhodobacter capsulatus* and isolation of a delta-aminolevulinic acid-dependent mutant strain. Mol. Gen. Genet. **221:**371–378.
21. **Jordan, P. M.** 1990. Biosynthesis of 5-aminolevulinic acid and its transformation into coproporphyrinogen in animals and bacteria, p. 55–121. *In* H. A. Dailey (ed.), Biosynthesis of hemes and chlorophylls. McGraw-Hill, New York.
22. **Lascelles, J.** 1978. Regulation of pyrrole synthesis, p. 795–808. *In* R. K. Clayton and W. R. Sistrom (ed.), The photosynthetic bacteria. Plenum Press, New York.
23. **Lee, J. K., and S. Kaplan.** 1992. *cis*-acting regulatory elements involved in oxygen and light control of *puc* operon transcription in *Rhodobacter sphaeroides*. J. Bacteriol. **174:**1146–1157.
24. **Lee, J. K., P. J. Kiley, and S. Kaplan.** 1989. Posttranscriptional control of *puc* operon expression of B800-850 light-harvesting complex formation in *Rhodobacter sphaeroides*. J. Bacteriol. **171:**3391–3405.
25. **Leong, S. A., G. S. Ditta, and D. R. Helinski.** 1982. Heme biosynthesis in *Rhizobium*. Identification of a cloned gene coding for 5-aminolevulinic acid synthetase from *Rhizobium meliloti*. J. Biol. Chem. **257:**8724–8730.
26. **Leong, S. A., P. H. Williams, and G. S. Ditta.** 1985. Analysis of the 5′ regulatory region of the gene for δ-aminolevulinic acid synthetase of *Rhizobium meliloti*. Nucleic Acids Res. **13:**5965–5976.
27. **Leuking, D. R., R. T. Fraley, and S. Kaplan.** 1978. Intracytoplasmic membrane synthesis in synchronous cell populations of *Rhodopseudomonas sphaeroides*. J. Biol. Chem. **253:**451–457.
28. **Lipman, D. J., and W. R. Pearson.** 1985. Rapid and sensitive protein similarity searches. Science **227:**1435–1441.
29. **Maguire, D. J., A. R. Day, I. A. Borthwick, G. Srivastava, P. L. Wigley, B. K. May, and W. H. Elliott.** 1986. Nucleotide sequence of the chicken 5-aminolevulinate synthase gene. Nucleic Acids Res. **14:**1379–1391.
30. **Maniatis, T., E. F. Fritsch, and J. Sambrook.** 1982. Molecular cloning: a laboratory manual. Cold Spring Harbor Laboratory, Cold Spring Harbor, N.Y.
31. **Marceau, M., S. D. Lewis, C. L. Kojiro, K. Mountjoy, and J. A. Shafer.** 1990. Disruption of active site interactions with pyridoxal 5′-phosphate and substrates by conservative replacements in the glycine-rich loop of *Escherichia coli* D-serine dehydratase. J. Biol. Chem. **265:**20421–20429.
32. **McClung, C. R., J. E. Somerville, M. L. Guerinot, and B. K. Chelm.** 1987. Structure of the *Bradyrhizobium japonicum* gene *hemA* encoding 5-aminolevulinic acid synthase. Gene **54:**133–139.
33. **McKnight, S. L., and R. Kingsbury.** 1982. Transcriptional control signals of a eukaryotic protein-coding gene. Science **271:**316–324.
34. **Messing, J.** 1979. A multipurpose cloning system based on single-stranded DNA bacteriophage M13. Recomb. DNA Tech. Bull. **2:**43–48.
35. **Michalski, W. P., and D. J. D. Nicholas.** 1987. Inhibition of bacteriochlorophyll synthesis in *Rhodobacter sphaeroides* subsp. *denitrificans* grown in light under denitrifying conditions. J. Bacteriol. **169:**4651–4659.
36. **Nandi, D. L., and D. Shemin.** 1977. Quaternary structure of δ-aminolevulinic acid synthase from *Rhodopseudomonas spheroides*. J. Biol. Chem. **252:**2278–2280.
37. **Neidle, E. L., and S. Kaplan.** 1992. 5-Aminolevulinic acid availability and control of spectral complex formation in HemA and HemT mutants of *Rhodobacter sphaeroides*. J. Bacteriol. **175:**2304–2313.
38. **Neidle, E. L., and S. Kaplan.** 1992. *Rhodobacter sphaeroides rdxA*, a homolog of *Rhizobium meliloti fixG*, encodes a membrane protein which may bind cytoplasmic [4Fe-4S] clusters. J. Bacteriol. **174:**6444–6454.

38a. **Neidle, E. L., and S. Kaplan.** Unpublished data.

39. **Neuberger, A., J. D. Sandy, and G. H. Tait.** 1973. Control of 5-aminolevulinate synthetase activity in *Rhodopseudomonas sphaeroides*. The involvement of sulfur metabolism. Biochem. J. **136:**477–490.
40. **Otsuka, A. J., M. R. Buoncristiani, P. K. Howard, J. Flamm, C. Johnson, R. Yamamoto, K. Uchida, C. Cook, J. Ruppert, and J. Matsuki.** 1988. The *Escherichia coli* biotin biosynthetic enzyme sequences predicted from the nucleotide sequence of the *bio* operon. J. Biol. Chem. **263:**19577–19585.
41. **Prentki, P., and H. M. Krisch.** 1984. In vitro insertional mutagenesis with a selectable DNA fragment. Gene **29:**303–313.
42. **Sandy, J. D., R. C. Davies, and A. Neuberger.** 1975. Control of 5-aminolaevulinate synthase activity in *Rhodopseudomonas sphaeroides*: a role for trisulphides. Biochem. J. **150:**245–251.
43. **Sanger, F., S. Nicklen, and A. R. Coulson.** 1977. Nucleotide sequencing with chain-terminating inhibitors. Proc. Natl. Acad. Sci. USA **74:**5463–5467.
44. **Sarmientos, P., J. E. Sylvester, S. Contente, and M. Cashel.** 1983. Differential stringent control of the tandem *E. coli* ribosomal RNA promoters from the *rrnA* operon expressed *in vivo* in multicopy plasmids. Cell **32:**1337–1346.
45. **Schoenhaut, D. S., and P. J. Curtis.** 1986. Nucleotide sequence of mouse 5-aminolevulinic acid synthase cDNA and expression of its gene in hepatic and erythroid tissues. Gene **48:**55–63.
46. **Shine, J., and L. Dalgarno.** 1975. Determination of cistron specificity in bacterial ribosomes. Nature (London) **254:**34–38.

46a. **Spiro, S., and J. R. Guest.** 1990. FNR and its role in oxygen-regulated gene expression in *Escherichia coli*. FEMS Microbiol. Rev. **75**:399–428.
47. **Tai, T.-N., M. D. Moore, and S. Kaplan.** 1988. Cloning and characterization of the 5-aminolevulinate synthase gene(s) from *Rhodobacter sphaeroides*. Gene **70**:139–151.
48. **Tuboi, S., and S. Hayasaka.** 1972. Control of δ-aminolevulinate synthetase activity in *Rhodopseudomonas sphaeroides*. II. Requirements of a disulfide compound for the conversion of the inactive form of fraction I to the active form. Arch. Biochem. Biophys. **150**:690–697.
49. **Urban-Grimal, D., C. Volland, T. Garnier, P. Dehoux, and R. Labbe-Bois.** 1986. The nucleotide sequence of the HEM1 gene and evidence for a precursor form of the mitochondrial 5-aminolevulinate synthase in *Saccharomyces cerevisiae*. Eur. J. Biochem. **156**:511–519.
50. **van Niel, C. B.** 1944. The culture, general physiology, and classification of the non-sulfur purple and brown bacteria. Bacteriol. Rev. **8**:1–118.
51. **Vieira, J., and J. Messing.** 1982. The pUC plasmids, and M13mp7-derived system for insertion mutagenesis and sequencing with synthetic universal primers. Gene **19**:259–268.
52. **Warnick, G. R., and B. F. Burnham.** 1971. Regulation of porphyrin biosynthesis: purification and characterization of δ-aminolevulinic acid synthetase. J. Biol. Chem. **246**:6880–6885.
53. **Weinstein, J. D., and S. I. Beale.** 1983. Separate physiological roles and subcellular compartments for two tetrapyrrole biosynthetic pathways in *Euglena gracilis*. J. Biol. Chem. **258**:6799–6807.
54. **Wierenga, R. K., and W. G. J. Hol.** 1986. Prediction of the occurrence of the ADP-binding βαβ-fold in proteins, using an amino acid sequence fingerprint. J. Mol. Biol. **187**:101–107.
55. **Wright, M. S., J. J. Eckert, S. W. Biel, and A. J. Biel.** 1991. Use of a *lacZ* fusion to study transcriptional regulation for the *Rhodobacter capsulatus hemA* gene. FEMS Microbiol. Lett. **78**:339–342.
56. **Yamamoto, M., S. Kure, J. D. Engel, and K. Hiraga.** 1988. Structure, turnover, and heme-mediated suppression of the level of mRNA encoding rat liver delta-aminolevulinate synthase. J. Biol. Chem. **263**:15973–15979.
57. **Yang, D., Y. Oyaizu, H. Oyaizu, G. J. Olsen, and C. R. Woese.** 1985. Mitochondrial origins. Proc. Natl. Acad. Sci. USA **82**: 4443–4447.
58. **Yanisch-Perron, C., J. Vieira, and J. Messing.** 1985. Improved M13 cloning vectors and host strains: nucleotide sequences of the M13mp18 and pUC19 vectors. Gene **33**:103–119.
59. **Yubisui, T., and Y. Yoneyama.** 1972. δ-aminolevulinic synthetase of *Rhodopseudomonas sphaeroides*: purification and properties of the enzyme. Arch. Biochem. Biophys. **150**:77–85.
60. **Zhu, Y. S., and S. Kaplan.** 1985. Effects of light, oxygen, and substrates on steady-state levels of mRNA coding for ribulose 1,5-bisphosphate carboxylase and light-harvesting and reaction center polypeptides in *Rhodopseudomonas sphaeroides*. J. Bacteriol. **162**:925–932.